

Improving the performance of colloidal quantum-dot-sensitized solar cells

Sixto Giménez¹, Iván Mora-Seró^{1,4}, Lorena Macor¹,
Nestor Guijarro², Teresa Lana-Villarreal², Roberto Gómez²,
Lina J Diguna³, Qing Shen³, Taro Toyoda^{3,4} and Juan Bisquert¹

¹ Photovoltaic and Optoelectronic Devices Group, Departament de Física, Universitat Jaume I, E-12071 Castelló, Spain

² Departament de Química-Física i Institut Universitari d'Electroquímica, Universitat d'Alacant, Apartado 99, E-03080 Alacant, Spain

³ Department of Applied Physics and Chemistry, The University of Electro-Communications, 1-5-1 Chofugaoka, Chofu, Tokyo 182-8585, Japan

E-mail: sero@fca.uji.es and toyoda@pc.uec.ac.jp

Received 3 March 2009, in final form 5 May 2009

Published 1 July 2009

Online at stacks.iop.org/Nano/20/295204

Abstract

Solar cells based on a mesoporous structure of TiO₂ and the polysulfide redox electrolyte were prepared by direct adsorption of colloidal CdSe quantum dot light absorbers onto the oxide without any particular linker. Several factors cooperate to improve the performance of quantum-dot-sensitized solar cells: an open structure of the wide bandgap electron collector, which facilitates a higher covering of the internal surface with the sensitizer, a surface passivation of TiO₂ to reduce recombination and improved counter electrode materials. As a result, solar cells of 1.83% efficiency under full 1 sun illumination intensity have been obtained. Despite a relatively large short circuit current ($J_{sc} = 7.13 \text{ mA cm}^{-2}$) and open circuit voltage ($V_{oc} = 0.53 \text{ V}$), the colloidal quantum dot solar cell performance is still limited by a low fill factor of 0.50, which is believed to arise from charge transfer of photogenerated electrons to the aqueous electrolyte.

 Supplementary data are available from stacks.iop.org/Nano/20/295204

(Some figures in this article are in colour only in the electronic version)

1. Introduction

Nowadays, there exists an intense effort aimed at developing third-generation solar cells. One of the most promising approaches involves the use of semiconductor quantum dots (QDs) as light absorbers. QDs exhibit attractive characteristics as sensitizers due to their tunable bandgap [1] by size control, which can be used to match the absorption spectrum to the spectral distribution of solar light. Additionally, QDs possess higher extinction coefficients [1, 2], compared to metal-organic dyes, and large intrinsic dipole moment leading to rapid charge separation [3, 4]. The demonstration of multiple exciton generation by impact ionization [5, 6] has fostered interest in colloidal quantum dots. One of the most attractive configurations to exploit these fascinating properties

of QDs is the quantum-dot-sensitized solar cell (QDSC) [7, 8]. The optimization of QDSCs can benefit from the intensive effort carried out with dye-sensitized solar cells (DSCs) [9]. Nevertheless the use of QDs as light absorbers requires the development of new strategies in order to push up the performance of QDSCs. Two main different approximations have been employed to sensitize with QDs a wide gap nanostructured semiconductor electrode (TiO₂, ZnO): (1) direct growth of the semiconductor QDs on the electrode surface by chemical reaction of ionic species using the methods of chemical bath deposition (CBD) [10–12] or successive ionic layer adsorption and reaction (SILAR) [13, 14] and (2) using presynthesized colloidal QDs attached to the electrode material by a bifunctional linker molecule [15–19]. Presynthesized colloidal QDs constitute an absorber material with tailored and well-controlled morphological characteristics

⁴ Authors to whom any correspondence should be addressed.

(shape and size), which could be an excellent building block for the development of more sophisticated structures with enhanced properties. However, at present, the use of presynthesized colloidal QDs leads to less efficient solar cell devices compared to directly grown QDs. In these devices, the role of the linker molecule is crucial for its performance [15, 18, 19]. Bifunctional molecular linkers have been systematically employed to attach colloidal CdSe QDs to a wide gap nanostructured semiconductor electrode since only weak direct adsorption (DA) of QDs is observed when dispersed in toluene [20]. These bifunctional linkers exhibit a carboxylic group that attaches to TiO₂ and a thiol group that attaches to the QD by ligand exchange, replacing the TOP capping molecules and linking the QDs directly to the TiO₂ surface [15, 18]. It is believed that the spatial separation between QDs and the electrode material reduces electron tunnelling injection [21] and has been considered as the main reason for the lower photocurrents obtained in these devices, lower than 4 mA cm⁻² under one sun illumination [18, 20, 22]. In the present study, we take advantage of a new strategy for adsorbing presynthesized colloidal CdSe QDs without the aid of any molecular linker, significantly increasing the obtained photocurrents [19]. Although QD direct adsorption has already been employed to sensitize TiO₂ with CdSe [23], InAs [24] and InP [25], the obtained photocurrents at one sun intensity were limited. CdSe colloidal QDs capped with trioctylphosphine and dissolved in dichloromethane (CH₂Cl₂) were directly adsorbed on nanoporous TiO₂ electrodes as light harvesting material for photovoltaic conversion. The roles of particle size distribution in the nanostructured TiO₂ film, adsorption time, surface passivation by a ZnS coating and counter electrode material on the solar cell performance were evaluated. These studies have led to a cell performance: $J_{sc} = 7.13 \text{ mA cm}^{-2}$, $V_{oc} = 0.53 \text{ V}$, $FF = 0.48$ and efficiency = 1.83% under full one sun illumination intensity. This is, to the best of our knowledge, the highest efficiency ever reported for solar cells employing presynthesized colloidal CdSe quantum dots.

2. Experimental details

2.1. Preparation of CdSe QDs

CdSe QDs, capped with trioctylphosphine (TOP) and dispersed in toluene, were prepared by a solvothermal route that allows size control [26]. Briefly, selenium reacts with cadmium myristate in toluene in the presence of oleic acid and TOP. The reaction takes place at 180 °C in a sealed autoclave. The QD size depends on reaction time; for the QDs used in this work the reaction time was 15 h. The synthesized QDs are characterized by a well-defined peak at 550 nm (first excitonic peak), which reveals a narrow size (diameter) distribution around $3.0 \pm 0.1 \text{ nm}$ [1]. For DA of QDs onto TiO₂ surface, solvent substitution is needed and a CH₂Cl₂ (99.6%, Sigma Aldrich) CdSe QD dispersion was prepared by centrifugation of the toluene colloidal dispersion and redissolution.

2.2. Preparation of QD-sensitized electrodes

A compact layer of TiO₂ (thickness ~100–200 nm) was deposited by spray pyrolysis of an aerosol of titanium(IV)

bis(acetoacetonato) di(isopropanoxylate) (Sigma Aldrich) onto the SnO₂:F (FTO)-coated glass electrodes (Pilkington TEC15, 15 Ω/sq resistance). The FTO electrodes were kept at 400 °C during spraying to burn off all the organics, thus leaving behind a compact layer of TiO₂. Subsequently, the coated substrate was fired at 450 °C for 30 min. Two colloidal TiO₂ pastes with different particle size distributions were deposited on top of the TiO₂ compact layer: a 350–450 nm particle size paste (paste A) was supplied by Dyesol (Queanbeyan, Australia) under the commercial name 18NR-AO and a 20–400 nm particle size paste (paste B) was supplied by ECN (Petten, The Netherlands). Around 0.25 cm² TiO₂ films were deposited by the doctor blade technique and subsequently sintered at 450 °C for 30 min in a muffle-type furnace. The thickness of the sintered TiO₂ films was approximately 10 μm measured by a Dektack 6 profilometer from Veeco. The TiO₂ photoanodes were directly immersed in the QD dispersion for different times ranging from 1 to 168 h. Some electrodes were coated with ZnS by twice dipping alternately into 0.1 M Zn(CH₃COO)₂ and 0.1 M Na₂S solutions for 1 min/dip, rinsing with Milli-Q ultrapure water between dips [27]. To compare the results with electrodes sensitized with QDs using cysteine as a bifunctional linker, some cells have been prepared using the procedure described in [18]. In this case, no change in the cell performance has been observed after adsorption times longer than 48 h.

2.3. Solar cell configuration

Two types of solar cell configuration were employed in the present study. The cells used in the study of different adsorption times (figures 1–3) were prepared by sealing the counter electrode and the QD-sensitized FTO/TiO₂ electrode using a thermoplastic spacer (DuPont™ Surlyn® 1702, thickness 50 μm). The polysulfide Na₂S_x redox electrolyte was prepared following the procedure described in [28]: it was a 1 M Na₂S, 0.1 M S and 0.1 M NaOH solution in Milli-Q ultrapure water. The electrolyte was introduced into the sealed cell through a hole pre-drilled in the counter electrode, which was sealed after filling. The rest of the cells were prepared by assembling the counter electrode and a QD-sensitized FTO/TiO₂ electrode using a silicone spacer (thickness 50 μm) and with a droplet (10 μl) of polysulfide electrolyte (identical to that described above, but with 1 M S).

2.4. Optical and electrical characterization

The absorption spectra were recorded by a Shimadzu UV-2401 PC. Current–potential curves were obtained using a FRA-equipped PGSTAT-30 from Autolab (figures 1 and 3) and a Keithley 2612 system sourcemeter® (figures 4(b) and 5). The cells were illuminated using a solar simulator at AM 1.5 G, where the light intensity was adjusted with an NREL-calibrated Si solar cell with a KG-5 filter to one sun intensity (100 mW cm⁻²). The IPCE measurements shown in figure 2 were performed employing a 150 W Xe lamp coupled with a monochromator controlled by a computer; the photocurrent was measured using an optical power meter 70310 from Oriel Instruments. At least two cells were tested at each condition to

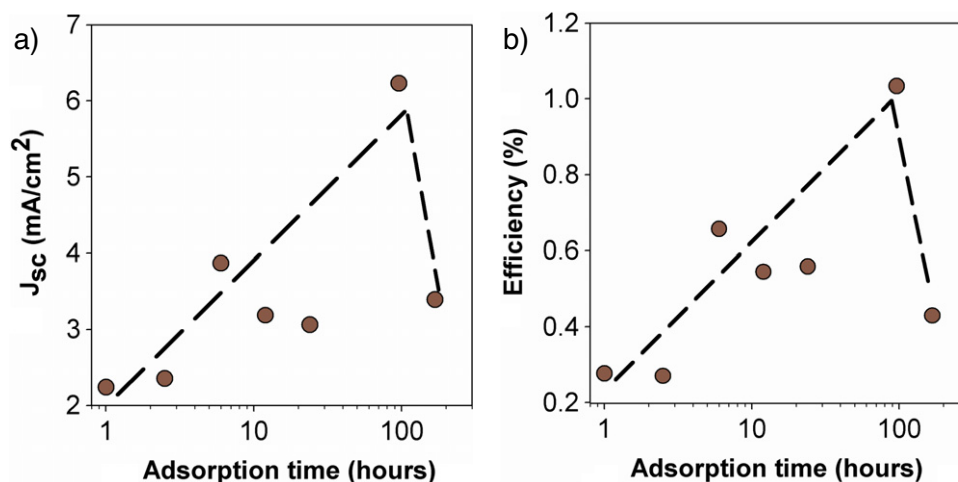


Figure 1. Time evolution of the performance of QDSC under one sun illumination: (a) J_{sc} , (b) efficiency. Cell configuration: FTO + compact TiO_2 + nanoporous TiO_2 + CdSe + polysulfide electrolyte (0.1 M S) + Pt counter electrode. Dashed lines are plotted as guides for the eyes.

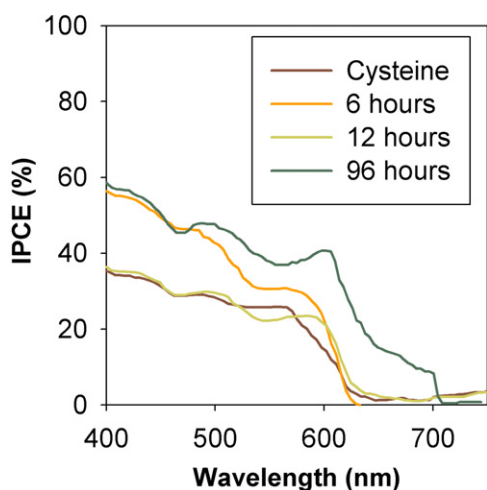


Figure 2. Evolution of IPCE with adsorption time. Comparison with a cell sensitized with QDs dissolved in toluene (using cysteine as a molecular linker with 24 h adsorption time) is also reported. Cell configuration: FTO + compact TiO_2 + nanoporous TiO_2 + CdSe + polysulfide electrolyte (0.1 M S) + Pt counter electrode.

validate the obtained trends. These measurements have been corrected considering the reflection in the glass/FTO substrate. IPCE measurements in figure 4 were carried out using a 300 W Xe arc lamp and equipped with a monochromator G-250 from Nikon and a zero-shunt meter NZ-1 from Nikko instruments.

2.5. Counter electrodes

Two kinds of Pt counter electrodes have been used: for sealed cells a thermally platinumized FTO counter electrode and a 200 nm thick platinum-sputtered FTO glass for cells using silicone spacer. The Au counter electrodes were prepared by sputtering Au-Pd alloy onto an FTO substrate. The Cu_2S counter electrodes were prepared by immersing brass in HCl solution at 70 °C for 5 min and subsequently dipping it into

Table 1. Photovoltaic properties of sealed QDSC under one sun illumination (AM 1.5 G). Cells have been sealed with Surlyn[®] and Pt has been used as the counter electrode.

TiO_2 paste/ adsorption time	V_{oc} (V)	J_{sc} (mA cm^{-2})	FF	η (%)
Paste A/24 h	0.44	3.06	0.42	0.56
Paste B/24 h	0.43	3.31	0.23	0.33
Paste A/96 h	0.49	6.23	0.34	1.03

polysulfide solution for 10 min, resulting in a porous Cu_2S electrode [29].

3. Results and discussion

Figure 1 shows the evolution of short circuit current (J_{sc}) and QDSC efficiency with QD adsorption time for sealed solar cells prepared with paste A (approx. 400 nm TiO_2 particles) and polysulfide redox electrolyte. Both quantities increase with adsorption time up to 96 h, peaking at 6.23 mA cm^{-2} and 1.03%, respectively (table 1), for the set of samples analysed. For linker-assisted adsorption using cysteine, the maximum cell performance was 0.71% ($J_{sc} = 3.95 \text{ mA cm}^{-2}$), using an Au counter electrode and a QD adsorption time of 48 h. No further increase in cell performance using the cysteine linker, which is the most efficient to date [18], has been obtained on increasing the QD adsorption time. This result indicates that DA allows a significant increase of the J_{sc} obtained from colloidal QDs. In a previous study, we showed that DA significantly increases the external quantum efficiency of the QD-sensitized electrodes compared to linker-assisted adsorption using mercaptopropionic acid (MPA) [19]. This fact clearly suggests that, when the QDs are directly attached to the surface, the electronic injection is favoured. It is believed that this mode of attachment involves a partial removal of the TOP layer at the contact points with the oxide particles and consequently the distance between the QD (electron donor) and the TiO_2 particle (electron acceptor) is reduced.

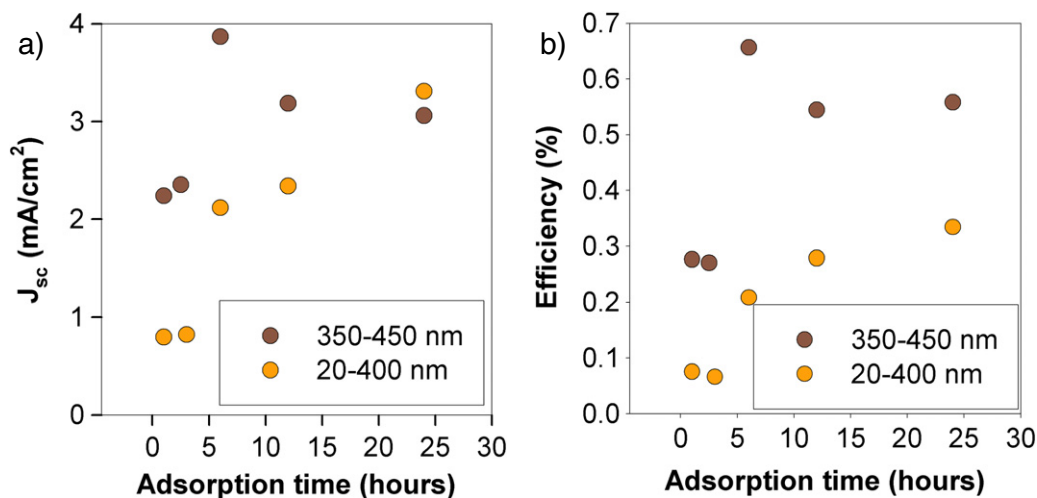


Figure 3. Effect of TiO₂ particle size distribution on the cell performance (under one sun illumination). Cell configuration: FTO + compact TiO₂ + nanoporous TiO₂ + CdSe + polysulfide electrolyte (0.1 M S) + Pt counter electrode.

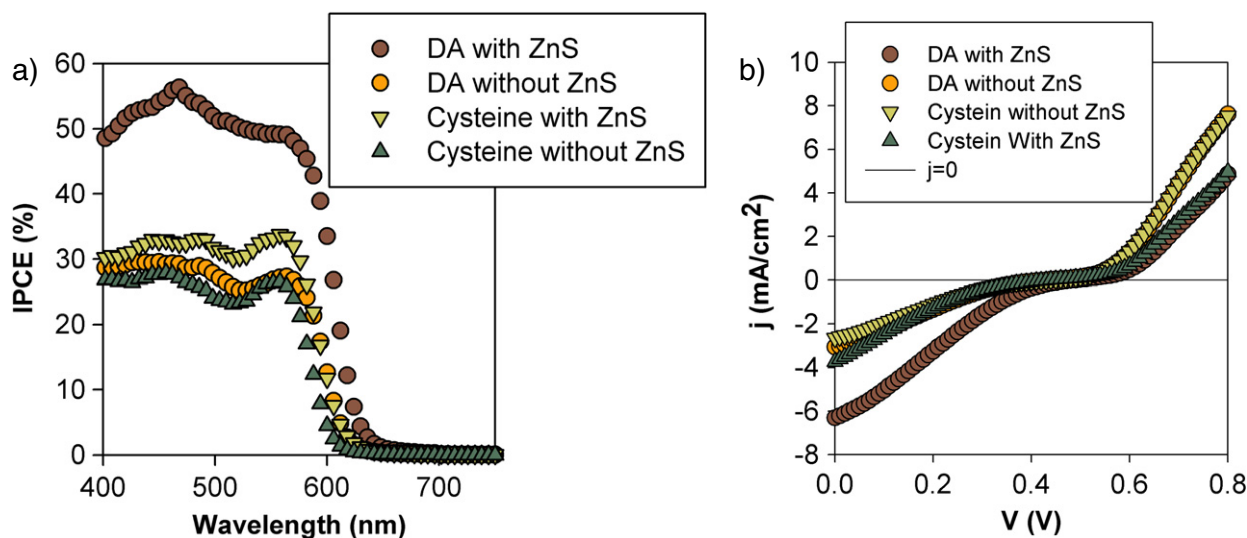


Figure 4. Effect of the ZnS passivation treatment on (a) IPCE and (b) current–potential curves under one sun illumination for a cell configuration: FTO + compact TiO₂ + nanoporous TiO₂ paste A + CdSe + polysulfide electrolyte (1 M S) + Pt counter electrode. QD adsorption time: 24 h.

Colloidal QD adsorption on TiO₂ surface in both DA and using bifunctional linkers depends on many factors (i.e. adsorption time, surface and solution cleanliness, QD concentration in the dispersion, type of TiO₂ paste (see below), surface treatments, etc) that are not completely optimized. They are, in any case, very difficult to control. To reduce the effect of these parameters, long adsorption times are generally used in order to obtain high QD loadings, such as 48 h [19] or 72 h [22] using the MPA linker. For DA, an excess increase of the adsorption time produces problems of agglomeration (see below), and due to the broad range of parameters affecting the adsorption process, a certain degree of dispersion of the results is observed when a set of measurements are carried out at different adsorption times, as is shown in figure 1 and in [19]. In this sense the DA process needs to be optimized, not only taking into account the adsorption time, in order to

obtain a maximum performance. However, figure 1 shows the potentialities of this method to obtain higher photocurrents. Further understanding of the adsorption process and the parameters that affect it would greatly contribute to improving the efficiency of this kind of cell, and higher performance could be anticipated.

Figure 2 shows the evolution of IPCE spectra with adsorption time for 6, 12 and 96 h at sealed cell configuration. These results are also compared with those using cysteine as a linker [18]. There is a systematic redshift with adsorption time (564 nm, 586 nm and 601 nm for 6, 12 and 96 h, respectively) for DA cells, pointing to a certain degree of QD agglomeration, with a concomitant deleterious effect for very long adsorption times [19], see figure 1. Such a deleterious effect could be observed for shorter adsorption times when P25 TiO₂ films were used. Since the particle size of P25 (15–80 nm) is smaller

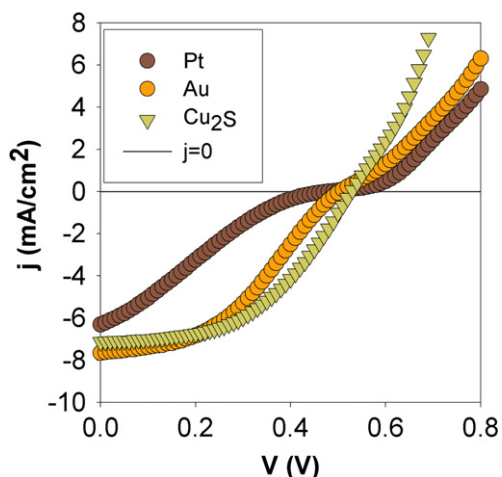


Figure 5. Current–potential curves (one sun) for different counter electrode materials (Pt, Au and Cu₂S). Cell configuration: FTO + compact TiO₂ + nanoporous TiO₂ paste A + CdSe + polysulfide electrolyte (1 M S) + counter electrode. QD adsorption time: 24 h.

than that of paste A by more than one order of magnitude, the present result provides the first illustration that using larger TiO₂ particle size is beneficial in this type of cell.

It is remarkable that the IPCE spectrum is importantly redshifted in the case of the 96 h electrode. The adsorption onset wavelength appears to be 700 nm, which is close to the value corresponding to the bandgap of bulk CdSe. This indicates a high degree of QD aggregation, to the point that the spectral behaviour of the CdSe does not resemble that of the dispersed QDs. In spite of this, the cells exhibit high IPCE values, indicating that aggregation is not necessarily deleterious as long as the nanochannels in the TiO₂ are not blocked. The latter was one of the reasons presented as explaining the important drop in IPCE occurring on P25 TiO₂ films for high CdSe QD adsorption times [19]. On the other hand, a 6 h adsorption time leads to higher IPCE values than 12 h adsorption time, as expected from the J_{sc} values plotted in figure 1. This is due to the dispersion of measurements previously commented on. The effect of the TiO₂ particle size distribution on the photovoltaic conversion performance is summarized in figure 3 and table 1. The experimental dispersion obtained for these results is presented as supplementary information (available at stacks.iop.org/Nano/20/295204). Higher photocurrents (figure 3(a)) and efficiencies (figure 3(b)) are systematically obtained for the larger particle size distribution (paste A), which correlates to a more open pore structure. An exception occurs for the photocurrent at 24 h adsorption time (see table 1 and figure 3(a)) attributed to statistical dispersion. Paste A is usually employed to prepare a scattering layer in conventional DSCs. From a rough estimate of the effective size of a QD adsorption unit (QDs + TOP) as 5 nm diameter (QD = 3 nm, TOP = 1 + 1 nm), it is clear that pore sizes below 10 nm may hinder the penetration of QDs into the nanoporous structure, leading to a reduction of the amount of adsorbed QDs. This limitation clearly illustrates

Table 2. Photovoltaic properties of closed QDSC under one sun illumination (AM 1.5 G). Cells were prepared using silicone spacer and paste A. QD adsorption time: 24 h.

w/wo ZnS/counter	V_{oc} (V)	I_{sc} (mA cm ⁻²)	FF	η (%)
Without ZnS/Pt	0.43	3.06	0.21	0.28
With ZnS/Pt	0.48	6.31	0.21	0.65
Without ZnS/Au	0.44	3.87	0.40	0.67
With ZnS/Au	0.50	7.65	0.42	1.60
With ZnS/Cu ₂ S	0.51	7.13	0.48	1.83

a significant difference with DSC, where maximum surface area is preferred for optimum performance. As an example, the effective size of the N3 dye molecule can be estimated as 1.6 nm [30]. The importance of the TiO₂ architecture on QD adsorption has been underlined previously [12, 22]. In a recent report [19], the fractional surface coverage of QDs on the TiO₂ surface, using Degussa P25, was estimated as 0.14. In this respect, alternative wide bandgap semiconductor architectures, enhancing accessible area and light scattering as inverse opal with surface area much lower compared to nanoparticulated films, have been demonstrated to provide an excellent substrate for efficient QD adsorption, leading to photovoltaic efficiencies close to 3% [12]. In this sense, optimization of wide bandgap semiconductor architecture is mandatory in order to increase QDSC performance.

The ZnS passivation treatment on nanostructured TiO₂ sensitized with CdSe QDs grown by CBD has been demonstrated to increase solar cell performance [12]. This treatment also increases dramatically both IPCE and photocurrent for colloidal QDs deposited by DA, as shown in figure 4 and table 2. A much lower increase in IPCE has been measured for colloidal QDs deposited using cysteine as the linker molecule (figure 4(a)), and consequently only a slight increase J_{sc} is observed in these cells after the ZnS treatment (figure 4(b)). For DA, IPCE, J_{sc} and efficiency are doubled, while V_{oc} and FF slightly increase or remain unchanged. IPCE values as high as 50% for the first excitonic peak have been found. The main reason for this higher performance is believed to rely on the increase of the recombination resistance between TiO₂ and the electrolyte [12, 31, 32]. When the same counter electrode material is used (figure 4(b)), the shape of the current density–potential (jV) curves is similar up to potentials close to V_{oc} . Conversely, at higher potentials, the recombination resistance (inverse of the slope of the IV curve) is reflecting the effect of the ZnS treatment. Independently of the type of QD adsorption (DA or linker-assisted), the charge transfer resistance takes values between 400–450 Ω cm² and 300–320 Ω cm² for specimens with and without the ZnS treatment, respectively. Consequently, the ZnS coating seems to passivate the TiO₂ surface, reducing recombination, rather than protecting the QDs.

It is well known that the electrocatalytic activity of Pt with a polysulfide electrolyte is not satisfactory for solar cell applications and alternative counter electrode materials with higher activity (e.g. CoS, Cu₂S) have been proposed [29]. The effect of the counter electrode material on the cell performance is illustrated in figure 5 and table 2 for CdSe-sensitized TiO₂ electrodes after ZnS treatment. The substitution of

the counter electrode material mainly affects the fill factor, as has been previously suggested [18]: Cu₂S (FF = 0.48) clearly outperforms Au (FF = 0.42) and Pt (FF = 0.21), involving an almost threefold increase in efficiency (1.83 versus 0.65%) with respect to Pt counter electrode cells. This is due to a reduction in the charge transfer resistance between the redox couple and the counter electrode. It is noteworthy that the FF obtained for sealed and closed cell (using spacer) configurations are not comparable (see tables 1 and 2). The use of a spacer does not allow an appropriate confinement of the electrolyte compared to sealed cells, and additional parallel recombination pathways could occur, reducing the FF, mainly when a Pt counter electrode is used. On the other hand, the use of a closed cell configuration increases the reproducibility and allows measuring the same sensitized electrode using different counter electrodes or after the ZnS treatment.

4. Conclusions

Colloidal CdSe QDs capped with TOP and dispersed in CH₂Cl₂ could be attached to the TiO₂ surface without the use of any bifunctional linker. The roles of both TiO₂ particle size distribution and adsorption time on the QDSC performance have been studied, revealing that open pore structures lead to higher photovoltaic conversion efficiencies. Combining the use of ZnS treatment and Cu₂S counter electrode leads to a cell performance of $J_{sc} = 7.13 \text{ mA cm}^{-2}$, $V_{oc} = 0.53 \text{ V}$, FF = 0.48 and efficiency = 1.83%, which is, to date, the highest reported efficiency for solar cells sensitized with presynthesized colloidal CdSe quantum dots. However, the cell is not fully optimized and better results can be anticipated.

Acknowledgments

This work was partially supported by the Ministerio de Educación y Ciencia and Ministerio de Exteriores y Cooperación of Spain under project HOPE CSD2007-00007 (Consolider-Ingenio 2010) and AECID CF101, respectively, and by Generalitat Valenciana under project GVPRE/2008/252. SG, IMS and NG acknowledge the Spanish Ministry of Science and Technology for its financial support through the Ramón y Cajal, Juan de la Cierva and FPU programs, respectively. Jan Kroon (ECN) is acknowledged for providing the TiO₂ paste B.

References

- [1] Yu W, Qu L H, Guo W Z and Peng X G 2003 *Chem. Mater.* **15** 2854
- [2] Wang P, Zakeeruddin S M, Moser J E, Humphry-Baker R, Comte P, Aranyos V, Hagfeldt A, Nazeeruddin M K and Grätzel M 2004 *Adv. Mater.* **16** 1806
- [3] Vogel R, Pohl K and Weller H 1990 *Chem. Phys. Lett.* **174** 241
- [4] Vogel R, Hoyer P and Weller H 1994 *J. Phys. Chem. B* **98** 3183
- [5] Schaller R D, Sykora M, Pietryga J M and Klimov V I 2006 *Nano Lett.* **6** 424
- [6] Trinh M T, Houtepen A J, Schins J M, Hanrath T, Piris J, Knulst W, Goossens A P L M and Siebbeles L D A 2008 *Nano Lett.* **8** 1713
- [7] Klimov V I 2006 *J. Phys. Chem. B* **110** 16827
- [8] Nozik A J 2002 *Physica E* **14** 115
- [9] Regan B O' and Grätzel M 1991 *Nature* **353** 737
- [10] Gorer S and Hodes G 1994 *J. Phys. Chem.* **98** 5338
- [11] Niitsoo O, Sarkar S K, Pejoux C, Rühle S, Cahen D and Hodes G 2006 *J. Photochem. Photobiol. A* **181** 306
- [12] Diguna L J, Shen Q, Kobayashi J and Toyoda T 2007 *Appl. Phys. Lett.* **91** 023116
- [13] Nicolau Y F, Dupuy M and Brunel M 1990 *J. Electrochem. Soc.* **137** 2915
- [14] Nicolau Y F 1985 *Appl. Surf. Sci.* **22/3** 1061
- [15] Robel I, Subramanian V, Kuno M and Kamat P V 2006 *J. Am. Chem. Soc.* **128** 2385
- [16] López-Luque T, Wolcott A, Xu L P, Chen S, Wen Z, Li J, Rosa E De la and Zhang J Z 2008 *J. Phys. Chem. C* **112** 1282
- [17] Leschkies S K, Divakar R, Basu J, Enache-Pommer E, Boercker J E, Carter C B, Kortshagen U R, Norris D J and Aydil E S 2007 *Nano Lett.* **7** 1793
- [18] Mora-Seró I, Giménez S, Moehl T, Fabregat-Santiago F, Lana-Villareal T, Gómez R and Bisquert J 2008 *Nanotechnology* **19** 424007
- [19] Guijarro N, Lana-Villareal T, Mora-Seró I, Bisquert J and Gómez R 2009 *J. Phys. Chem. C* **113** 4208
- [20] Lee H J, Yum J-H, Leventis H C, Zakeeruddin S M, Haque S A, Chen P, Seok S I, Grätzel M and Nazeeruddin M K 2008 *J. Phys. Chem. C* **112** 11600
- [21] Bakkens E P A M, Roest A L, Marsman A W, Jenneskens L W, Jong-van steensel L I de, Kelly J J and Vanmaekelbergh D 2000 *J. Phys. Chem. B* **104** 7266
- [22] Kongkanand A, Tvrđy K, Takechi K, Kuno M and Kamat P V 2008 *J. Am. Chem. Soc.* **130** 4007
- [23] Shen Y, Bao J, Dai N, Wu J, Gu F, Tao J C and Zhang J C 2009 *Appl. Surf. Sci.* **255** 3908
- [24] Yu P, Zhu K, Norman A G, Ferrere S, Frank A J and Nozik A J 2006 *J. Phys. Chem. B* **110** 25451
- [25] Zaban A, Micic O I, Gregg B A and Nozik A J 1998 *Langmuir* **14** 3153
- [26] Wang Q, Pan D, Jiang S, Ji X, An L and Jiang B 2006 *J. Cryst. Growth* **286** 83
- [27] Yang S M, Huang C H, Zhai J, Wang Z S and Jiang L 2002 *J. Mater. Chem.* **12** 1459
- [28] Zhao P, Zhang H, Zhou H and Yi B 2005 *Electrochim. Acta* **51** 1091
- [29] Hodes G, Manassen J and Cahen D 1980 *J. Electrochem. Soc.* **127** 544
- [30] Suryanarayanan V, Sreekumaran Nair A, Tom R T and Pradeep T 2004 *J. Mater. Chem.* **14** 2661
- [31] Lee Y L, Huang B M and Chien H T 2008 *Chem. Mater.* **20** 6903
- [32] Shen Q, Kobayashi J, Diguna L J and Toyoda T 2008 *J. Appl. Phys.* **103** 084304